Journal of
Composites Science

MDPI

Article

Nano Propolis, Zinc Oxide Nanoparticles, and Their Composites: A Novel Green Synthesis with Synergistic Antioxidant and Anticancer Properties

Shaimaa A. Salama [1], Ramadan R. Atta [2,*], Ensaf M. Khalil [1], Yasser F. Abdelaleim [3], Samah Abd-Eltawab [4], Ahmed A. Farghali [5], Doaa Essam [6], Dalal Hussien M. Alkhalifah [7], Wael N. Hozzein [8] and Rehab Mahmoud [6]

1 Special Food and Nutrition Department, Food Technology Research Institute, Agriculture Research Center, Giza 12619, Egypt
2 Department of Chemistry, Faculty of Science, Damietta University, Damietta 34517, Egypt
3 Department of Agricultural Microbiology, Faculty of Agriculture, Fayoum University, Fayoum 6354, Egypt
4 Food Science and Technology Department, Faculty of Agriculture, Fayoum University, Fayoum P.O. Box 63514, Egypt
5 Materials Science and Nanotechnology Department, Faculty of Postgraduate Studies for Advanced Sciences, Beni-Suef University, Beni-Suef 62511, Egypt
6 Department of Chemistry, Faculty of Science, Beni-Suef University, Beni-Suef 62511, Egypt
7 Department of Biology, College of Science, Princess Nourah bint Abdulrahman University, P.O. Box 84428, Riyadh 11671, Saudi Arabia
8 Botany and Microbiology Department, Faculty of Science, Beni-Suef University, Beni-Suef 62511, Egypt
* Correspondence: ramadanatta75@du.edu.eg; Tel.: +20-1099410653

Abstract: Nanoparticles of zinc oxide (ZnO NPs), propolis, and the ZnO–propolis composite (ZnO-P NCs) have been synthesized using a biomimetic approach. Zeta potential analysis and Fourier-transform infrared spectroscopy (FT-IR) proved the formation and stability of nanomaterials. Findings using X-ray diffraction (XRD), scanning electron microscopy (SEM), energy-dispersive X-ray spectroscopy (EDX), EDX-imaging, and transmission electron microscopy (TEM) demonstrated that the particle size of ZnO-P NCs was 9.70 nm. The antioxidant (DPPH radical scavenging) activity of synthesized nanomaterials was investigated. IC_{50} values of zinc oxide, propolis, and ZnO-P NCs nanoparticles were 2.75, 1.7, and 1.45 mg mL^{-1}, respectively. In addition, their selectivity and anticancer activity for cancer cell lines (Hela and MCF-7) and human normal (W138) cell lines were investigated. ZnO-P NCs were highly effective against the cell line for breast cancer with an IC_{50} value of 18 µg/mL, indicating its anticancer-promising potent cytotoxicity in breast cancer treatment, and 23 µg/mL against cervical cancer. In addition, the higher observed safety, antioxidant, and anticancer activities for synthesized ZnO-P NCs confirmed the synergistic effect of this combination. It was obtained that the specific mechanisms underlying the synergy effect between zinc oxide nanoparticles and nanopropolis in their composite formulation varied depending on the preparation method, ratio, and concentration of the components.

Keywords: propolis; green synthesis; ZnO nanoparticles; anticancer; antioxidant; DPPH; composite; synergistic effect

Citation: Salama, S.A.; Atta, R.R.; Khalil, E.M.; Abdelaleim, Y.F.; Abd-Eltawab, S.; Farghali, A.A.; Essam, D.; Alkhalifah, D.H.M.; Hozzein, W.N.; Mahmoud, R. Nano Propolis, Zinc Oxide Nanoparticles, and Their Composites: A Novel Green Synthesis with Synergistic Antioxidant and Anticancer Properties. *J. Compos. Sci.* **2023**, *7*, 480. https://doi.org/10.3390/jcs7110480

Academic Editor: Francesco Tornabene

Received: 3 October 2023
Revised: 19 October 2023
Accepted: 31 October 2023
Published: 20 November 2023

1. Introduction

The development of sustainable technology is highly dependent on nanoparticles (NPs). There are several chemical and physical methods for synthesizing NPs [1,2]. These methods can be rather pricey and often include using organic solvents and hazardous substances that pose a risk to both the environment and living things [3]. Therefore, biologically generated nanoparticles are a viable option because they are cheap, environmentally friendly, and safe [4]. Thus, a non-toxic method of producing and stabilizing

nanoparticles has been to use plants, bacteria, fungi, and natural extracts [5]. Using natural and plant extracts [6] offers several advantages compared to alternative methods of ecologically friendly synthesis [7]. Propolis (P) is a naturally occurring viscose complex mixture with diverse and complex chemical compositions [8] created by honeybees and obtained from the components of various plants. Propolis is a resinous complex mixture that honeybees collect primarily from tree buds, sap flows, and various botanical sources. Bees combine this resin with beeswax, pollen, and their enzymes to create propolis. Its chemical composition is highly complex and can vary depending on the botanical sources available to bees. It typically contains a mix of polyphenols, flavonoids, terpenes, steroids, amino acids, vitamins, and other bioactive compounds. Propolis serves essential functions within the hive and has garnered attention for its potential health benefits in human use. Its rich and varied chemical composition makes it a subject of ongoing scientific inquiry and a valuable resource in traditional and modern medicine [9–12]. Due to its possible therapeutic characteristics, propolis has been exploited for various objectives, including immunity-enhancing, anti-inflammatory, antihypertensive, antimicrobial, antioxidant, anti-ulcer, and antitumor activities [13–15]. Published work on propolis's composition and biological features revealed researchers' interest in propolis and its potential for creating new medications [16–18]. Propolis is a natural antioxidant that does not cause toxicity, unlike synthetic antioxidants such as propyl gallate, butylated hydroxytoluene (BHT), and butylated hydroxyanisole (BHA) [19,20], which have been avoided because of health concerns. However, its antioxidant mechanism is similar to vitamin C and BHT [21]. Its antioxidant activity is mainly attributed to its polyphenolic content [22]. On the other hand, propolis exhibits specific toxic actions on cancer cells, inhibiting tumor cells while having little or no effect on normal cells [23]. Moreover, It was reported that propolis reduces the toxic effects of anticancer drugs and potentiates their activity [24,25]. These cytotoxic mechanisms primarily include ANXA7, NF-B inhibition, the control of the p53 protein, the membrane of mitochondria regulation, and ROS [23]. Galangin, the most important flavonoid in propolis, triggers apoptosis and suppress melanoma cell proliferation in in vitro research [26]. Propolis inhibits the proliferation of cells by endoplasmic reticulum stress caspase activation, reducing mitochondrial membrane potential and apoptosis [27]. In addition, the excellent cytotoxic activity of propolis was observed against the cervical (HeLa cells) and breast cancer (MCF-7) [28–31].

Despite its multiple benefits, its benefit in the body is limited due to its insufficient water-soluble ability, further limiting its clinical applications [15]. Developing a stable formulation with the required characteristics has been challenging for propolis and has been solved using nanotechnology. It entails either nanosizing the propolis to decrease the size of its particles or combining it into different nanocarriers that serve as propolis delivery systems, enabling propolis to be delivered to the targets much more successfully, while zinc oxide nanoparticles are a unique example of nano minerals. They have garnered a lot of interest in biomedical applications because of their special plasmonic effects, ease of fabrication, inert nature, high biocompatibility, and potential functionality for various purposes [32]. They have excellent antioxidant properties in normal mammalian cells through the up-regulation of antioxidant enzyme activities and scavenging of reactive free radicals [33]. They also exhibit significant anticancer activity at low concentrations due to their high surface area and unique chemical and physical properties that greatly enhance their bioavailability. As a result, ZnO NPs have created a new pathway for the advancement of novel approaches for rapid cancer diagnosis and treatment [34–36] effectively [37]. Nano minerals, on the other hand, have recently emerged as a promising alternative to inorganic minerals in the medical field for both diagnosis and therapy [38,39].

Owing to propolis containing reducing agents and stabilizing biocompounds, it has a potential application in the green synthesis of metal NPs as selenium, iron, copper, and silver nanoparticles [40–45]. However, there is a lack of studies on producing ZnO NPs using propolis. The only available method used was the non-aqueous extract, chemicals, multiple procedures, and required instrumentation [45].

Hybrid materials with excellent biological activity [46–48] are now relevant and appealing to readers [46,49,50]. Combining nano minerals and natural compounds enhances their physical and functional properties and, thus, their activities. A synergistic effect was observed from the use of ZnO NPs and the propolis composite on the UV-blocking property and antioxidant and antibacterial activities [51] in meat-packing applications. Other synergistic effects were reported in their combinations of antibacterial [52] and antifungal [53] activities. However, surveying the literature revealed a lack of studies on the synergism between ZnO NPs and propolis concerning antioxidant and anticancer activities. Consequently, this study's primary objective was to develop an environmentally friendly method for synthesizing ZnO NPs and nano propolis in a solvent (water). In addition, a novel composite of these two nanomaterials was desired to be synthesized and characterized to assess the possible synergistic effect of this combination. The procedures used were compared to traditional physicochemical and green synthesis techniques (Scheme 1).

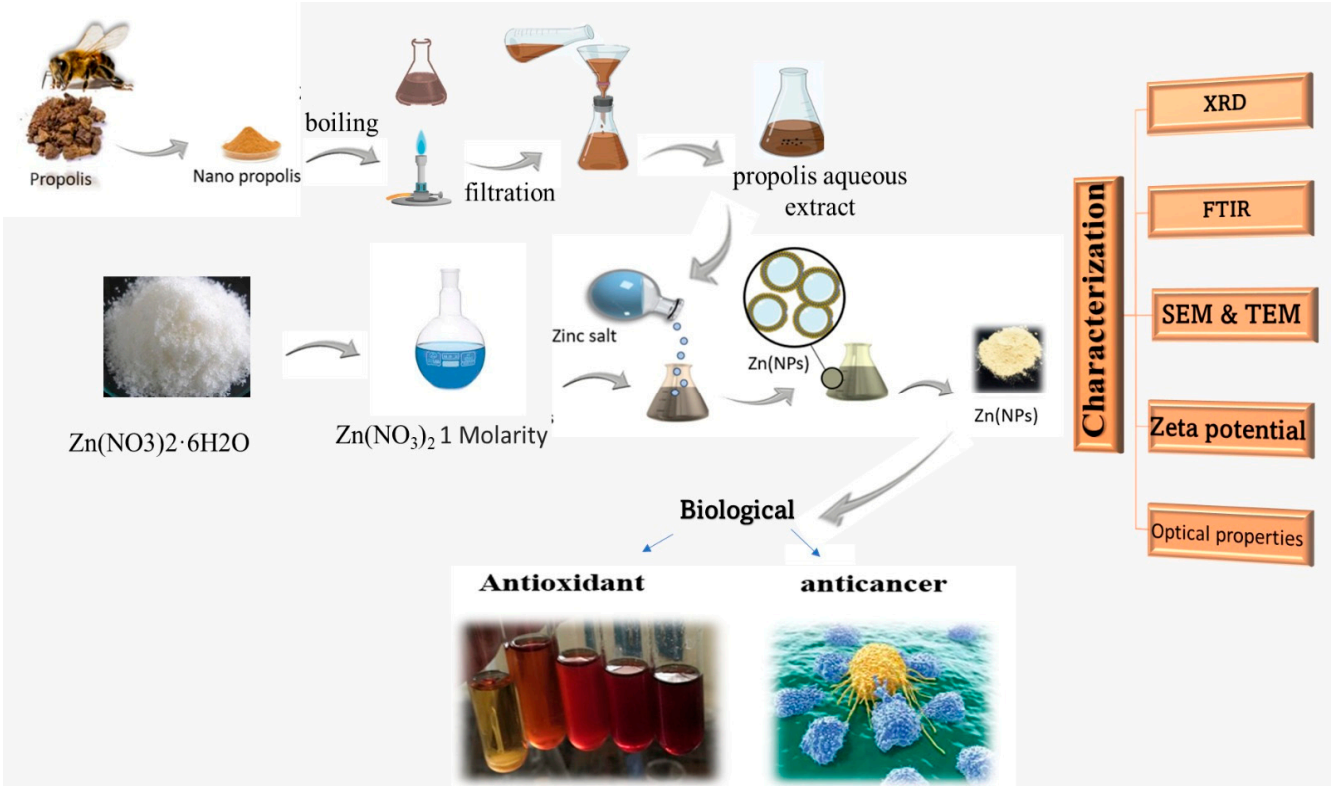

Scheme 1. Preparation of zinc oxide nanoparticles and their composites: their characterization and synergistic antioxidant and anticancer investigation.

2. Materials and Methods

All solutions were formulated using milli-Q water. Zinc nitrate ($Zn(NO_3)_2 \cdot 6H_2O$) was acquired from the Oxford Laboratory Reagent. Sodium hydroxide (NaOH), aluminum chloride ($AlCl_3$), and sodium nitrite ($NaNO_2$) were given by piochem to laboratory chemicals in Egypt and were used without additional purification. Folin–Ciocalteau reagent, gallic acid, 1,1-diphenyl-2-picrylhydrazyl (DPPH), the antioxidant ascorbic acid, 3-(4,5-dimethylthiazol-2-yl)-2,5-diphenyltetrazolium bromide, RPMI-1640 medium, dimethyl sulfoxide, catechin, and fetal bovine serum were all purchased from Sigma Aldrich (St. Louis, MO, USA). Sodium carbonate (Na_2CO_3) was available from el-nasr pharmaceutical chemicals in Cairo, Egypt. Carlo Erba reagent provided doxorubicin and hydrochloric acid (HCl). After ripening in August and October (seasons 2021), propolis was collected from honeybee (Apis mellifera) colonies reared in modern hives in tanta, el-gharbya governorate, Egypt.

2.1. Cell Lines

Epitheliod carcinoma cervix cancer (Hela), human lung fibroblast (WI38), and mammary gland breast cancer (MCF-7) were used. Through the holding company for biological products and vaccines (VACSERA), Cairo, Egypt, the cell line was obtained from ATCC (American Type Culture Collection).

2.2. Preparation of Nanoparticles

2.2.1. Propolis Nanoparticles Preparation

The propolis was subjected to a size reduction process to obtain nanoparticles using a top-down ball mill methodology as follows: The propolis was introduced into a stainless steel container containing a ceramic ball mill ranging in diameter from 1.11 to 1.75 cm at a propolis-to-ball mass ratio of 10:1. The entire setup was subjected to rotation utilizing ball mill equipment (Photon, Egypt) for 24 h, operating at 900 revolutions per minute (rpm). The resulting propolis was collected and investigated with different methods (Scheme 2).

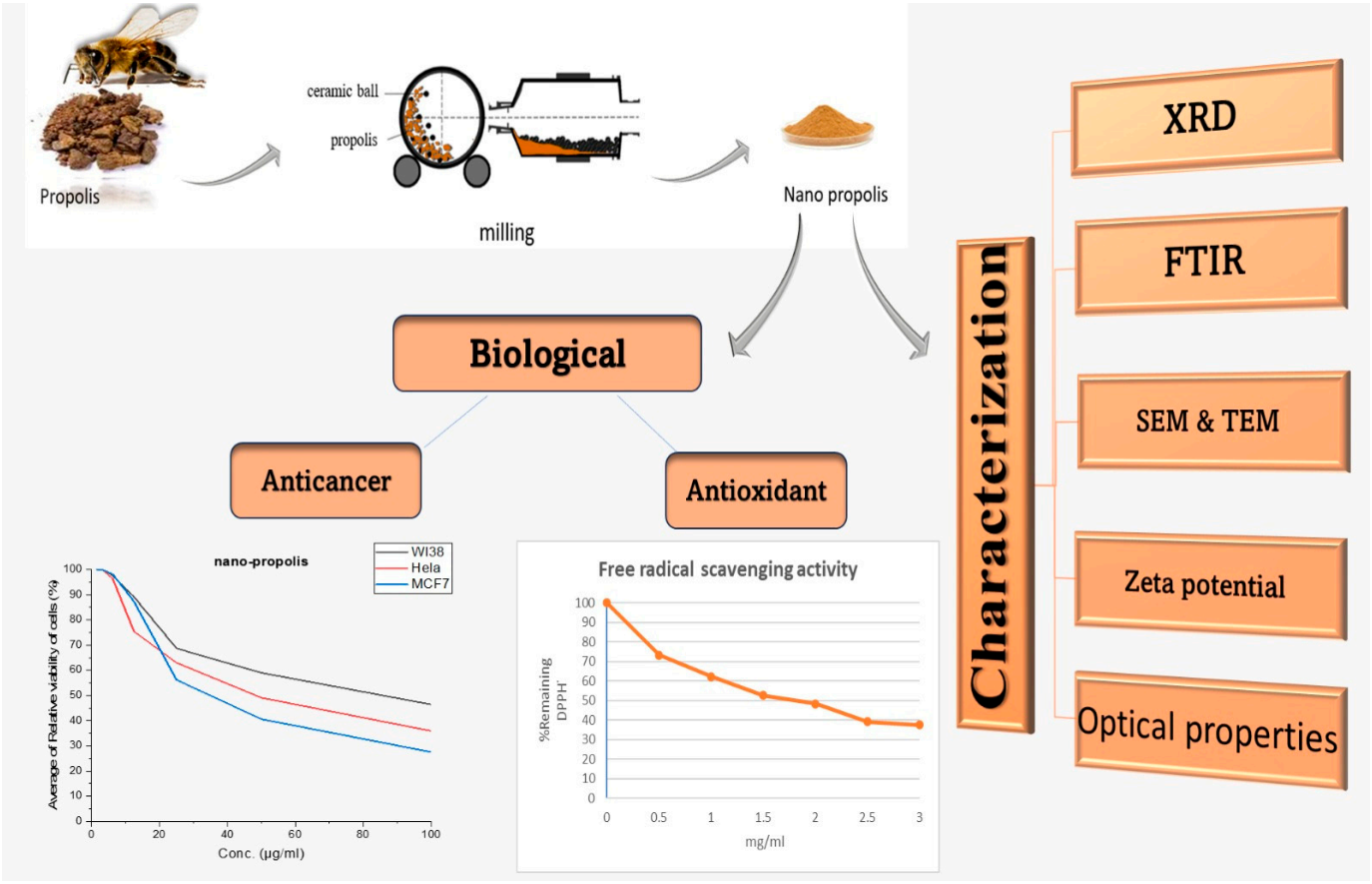

Scheme 2. Preparation and characterization of nano propolis.

The XRD analysis (Figure 1a,b) of propolis and nano propolis obtained only amorphous peaks. Nevertheless, the observed behaviors were different. The typical 2nd ETA angle at 22.35° of propolis appeared, but its intensity decreased in nano propolis and shifted to 21.23° [42]. This was probably due to the effect of the milling process. The surface morphology of the nano propolis was assessed using SEM imaging. As shown in Figure 1c, SEM images indicate that nano propolis has rough surface morphologies, suggesting an agglomeration of irregularly shaped particles. The particle size of nano propolis determined from SEM images of the particles ranged from 20 to 60 nm (Figure 1d).

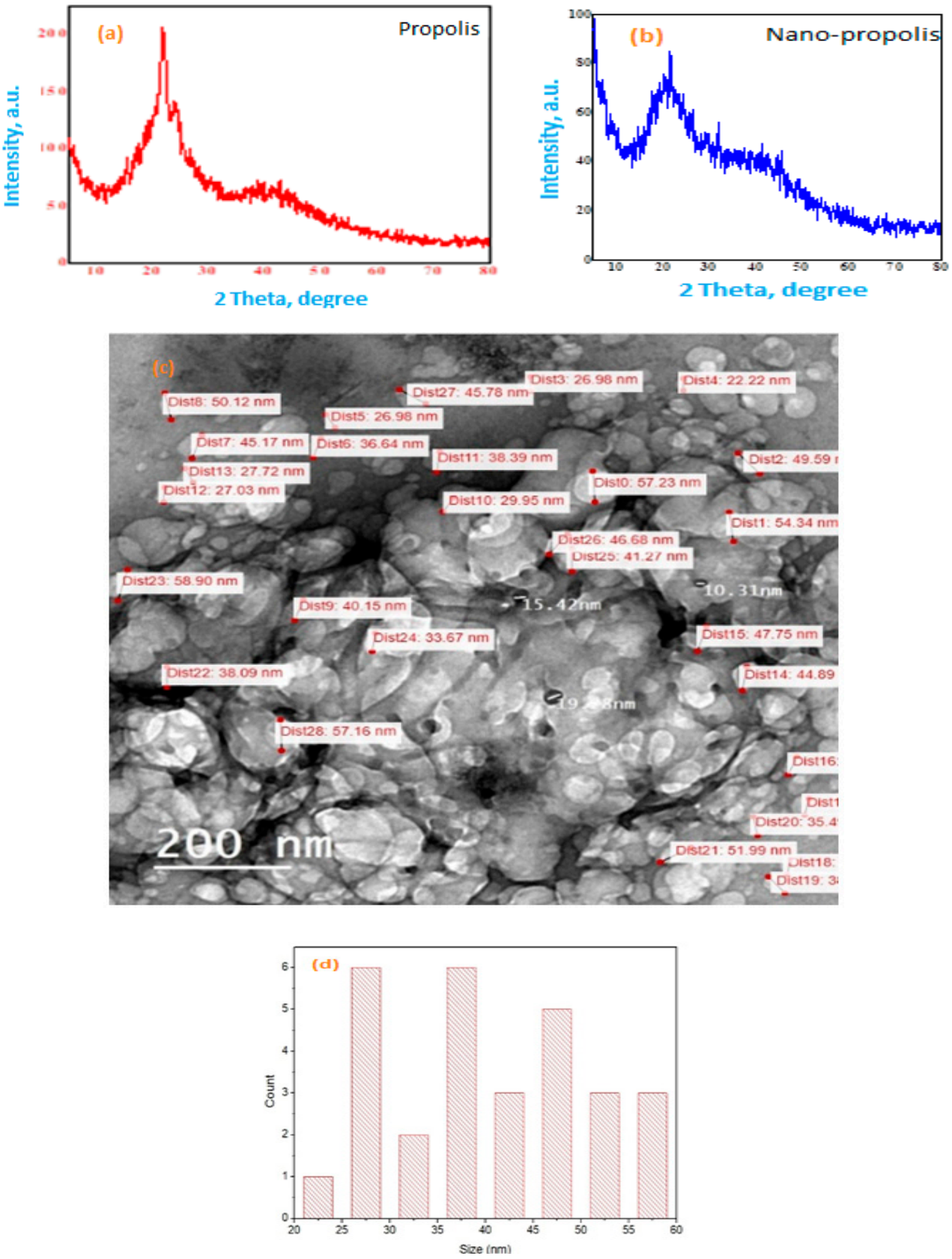

Figure 1. XRD pattern of propolis (**a**); nano propolis (**b**); SEM image of nano propolis (**c**); and partial size distribution of nano propolis (**d**).

2.2.2. Green Synthesis of Zn Oxide Nanoparticles Using Propolis

Zn oxide nanoparticles were prepared using a modified version of the coprecipitation approach described by Singh et al. [54]. In total, 20.0 g of propolis was added to 200 mL of milli-Q water at 100 °C for 10 min on a digital hot plate with a magnetic stirrer device. After cooling, the extract was centrifuged twice for 10 min at 4500 rpm, and the supernatant was filtered using Watman filter paper and stored at 4 °C for the green synthesis of Zn oxide nanoparticles.

A total of 0.10 M of the aqueous solution of zinc nitrate was used as the precursor. The composition of nitrate (Zn^{2+} solution) and the propolis extract in a 1:1 volume ratio was prepared by adding the propolis extract drop by drop to the zinc nitrate solution with constant stirring at 25 °C. The resulting particles were centrifuged twice for 20 min at 8000 rpm, then washed with bi-distilled water several times before the particles were dried at 100 °C. Zinc oxide nanoparticles were obtained in powder form (Scheme 3).

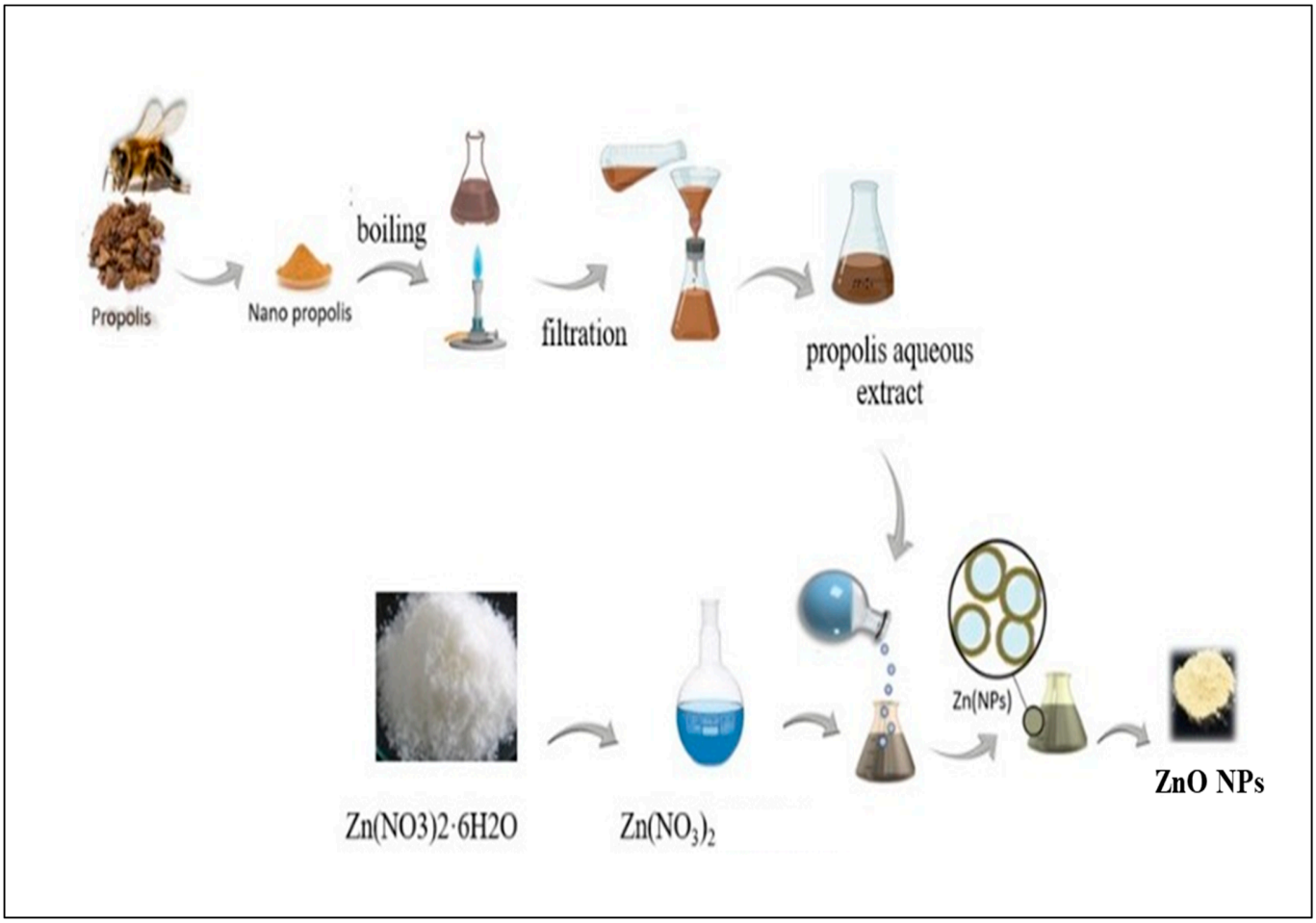

Scheme 3. Preparation of ZnO NPs using propolis extract.

2.2.3. Zinc Oxide–Propolis Nanocomposite (ZnO-P NCs) Preparation

ZnO-P NCs were prepared using a green synthesis approach with the propolis extract as follows: ZnO NPs were transferred to a beaker containing 5 g of nano propolis before the resultant mixture (suspension) was shaken for 24 h at 25°. After that, the mixture was centrifuged, and the residual supernatant was discarded. This step was repeated 4 additional times. The product obtained was then washed with 50 mL of ethanol (5 times). The obtained pure ZnO-P NCs were dried entirely at 100 °C and stored in an amber sample glass bottle at RT.

EDX analysis was conducted to confirm the presence of Zn, C, and Ca (Figure 2). EDX-mapping analysis (Figure 2) was also utilized to confirm the chemical composition and elemental distribution in our prepared material. Figure 2 presents homogeneous oxygen, carbon, and zinc distribution throughout the prepared ZnO-P NCs.

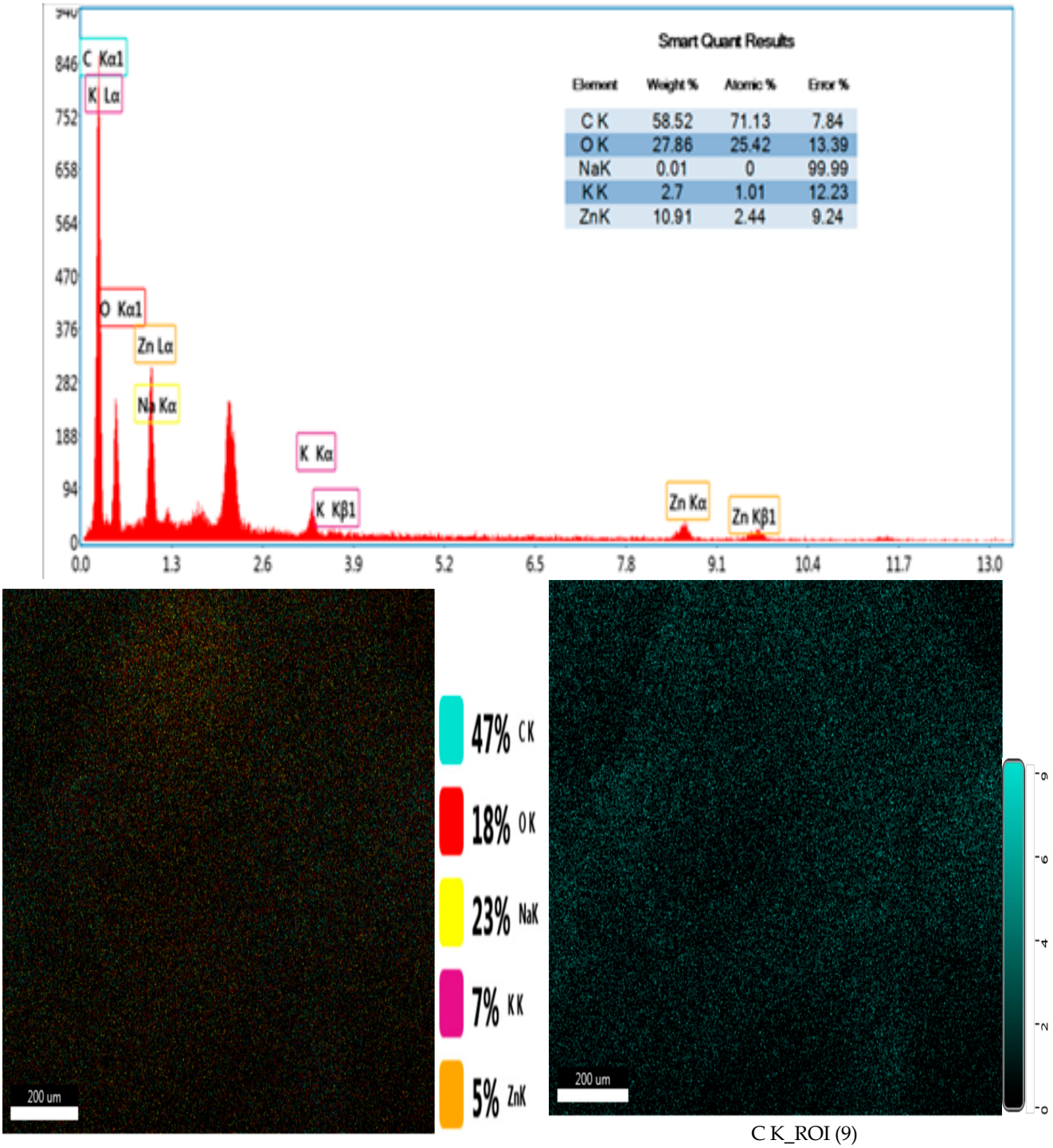

Figure 2. *Cont.*

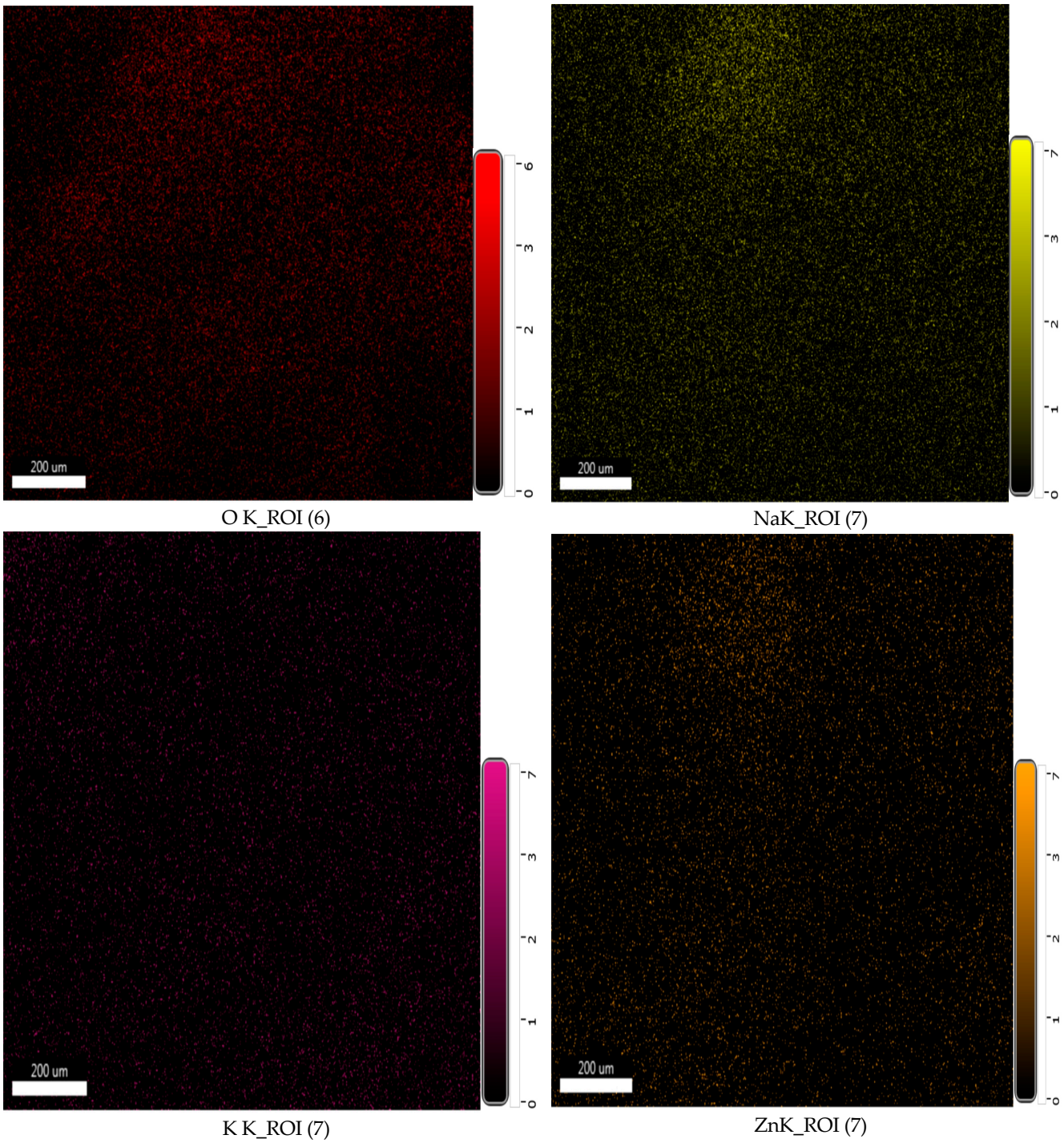

Figure 2. Energy-dispersive X-ray spectroscopy of synthesized ZnO-P NCs and EDX-mapping analysis.

2.3. Characterization

The PANalytical X-ray diffractometer (Empyrean) was utilized to conduct XRD analysis using Cu K radiation with a wavelength of 40 KV, a scanning rate of 0.02° min^{-1} from 0° to 80° (2θ), and operating the device at a current of 35 mA and an acceleration voltage of 40 kV. To conduct FTIR spectra, Bruker Vertex 70 was used. Field emission scanning electron microscopy (FESEM) and a scanning transmission electron microscope (STEM) were used to analyze the morphology of the synthesized nanoparticles. The microstructure and surface morphology of green ZnO NPs and ZnO-P NCs were studied using HRTEM (JEOL,

Tokyo, Japan, JEM-2100) at an accelerating voltage (200 KV). Zetasizer Nano (Malvern Instruments Ltd., Malvern, UK) assessed zeta potential and the hydrodynamic particle size. The method for preparing samples for zeta potential measurement was described in our earlier work [55]. The bandgap of the samples was calculated from the respective absorption edge using an Ultraviolet–visible spectrophotometer.

2.4. Total Phenolic and Flavonoid Contents Determination

The Folin–Ciocalteu technique measured the total phenolic contents of nano propolis and the synthetic nanoparticles (Meda, Lamien, Romito, Millogo, & Nacoulma, 2005) [56]. Aliquots of 0.1 g of lyophilized propolis powder and the synthesized nanoparticles were dissolved in 1 mL of distilled water. In total, 0.1 mL of this solution was mixed with 0.1 mL of the 50% Folin–Ciocalteau reagent, 2 mL of sodium carbonate (Na_2CO_3), and 2.8 mL of distilled water. After thirty minutes of incubation, the reaction mixture's absorbance at 750 nm was determined using a spectrophotometer (Hitachi, Tokyo, Japan; Model 100-20) against the distilled water blank. As a standard, gallic acid was used. Using the five-point standard curve (0–250 mg/L), the total phenolic contents in propolis and the synthesized nanoparticles were measured in triple. The calculation was expressed in milligrams of gallic acid equivalents ((GAE)/g). According to Chang, Yang, Wen, and Chern [57], the total flavonoid content was measured using the aluminum chloride colorimetric method. In 1 mL of distilled water, aliquots 0.1 g of the synthesized nanoparticles and propolis were separately dissolved. A total of 5 mL of the resultant solution was combined with 2.8 mL of distilled water, 1.5 mL of alcohol (95%), 0.1 mL of aluminum chloride ($AlCl_3$) (10%), and 0.1 mL of potassium acetate (CH_3COOK) (1 M). The reaction mixture's absorbance was measured at 415 nm against a distilled water blank using a spectrophotometer (Hitachi, Model 100-20) after a 40 min incubation period at room temperature. The standard was selected to be quercetin. Using the five-point standard curve (0–75 mg/L), the amounts of the total flavonoid content in the samples were measured in triplicate. It was presented in milligrams of quercetin equivalents (QE) per gram of lyophilized powder.

2.5. Antioxidant Activity (DPPH Assay)

The samples' antioxidant activity was examined using the DPPH• Colorimetric technique with the antioxidant agent ascorbic acid for comparison [58]. To prepare for the DPPH• solution, 25 mg of DPPH• was dissolved in 1000 mL of methanol. The DPPH• solution was mixed to the required final volume of 4 mL with samples at various concentrations. Every sample was diluted serially by mixing with methanol (0.5, 1, 1.5, 2, 2.5 mg/mL). In a test tube, 100 µL of each prepared sample was added to 3.9 mL of the DPPH• working solution. The samples with DPPH• solution were kept at room temperature for 30 min in the dark. Each sample's absorbance was determined at 515 nm using the following step.

The following equation was used to calculate the percentage of DPPH remaining:

$$\% \text{ DPPH• remaining} = [\text{DPPH•}]\ T/[\text{DPPH•}]T = 0 \times 100$$

The % DPPH• of the remaining values was graphed against mg nanomaterials/mL using an exponential curve to determine the inhibitory concentration "IC_{50}". The number of antioxidants needed to lower the initial concentration of the DPPH• solution by 50% is indicated by the IC_{50} value. The IC_{50} values correlate inversely with the investigated sample's antioxidant capability [59].

2.6. Anticancer Assay (MTT Assay)

The aforementioned cell lines were employed to evaluate the inhibitory effects of nano propolis, zinc oxide nanoparticles ZnO NPs, and their nanocomposites utilizing the MTT test to measure cell growth. In this colorimetric method, yellow tetrazolium bromide (MTT) was converted to a purple formazan derivative using the mitochondrial succinate dehydrogenase of live cells. Cell lines were cultured in an RPMI-1640 medium supplemented with 10% of fetal bovine serum. At 37 °C in an incubator with 5% CO_2,

antibiotics of 100 units/mL of penicillin and 100 µg/mL of streptomycin were introduced. The cell lines were seeded in a 96-well plate at 1.0 × 104 cells/well density and incubated with 5% CO_2 at 37 °C for 48 h. After incubation, the cells were exposed to various compound concentrations and incubated for 24 h. Following a 24 h drug treatment period, 20 µL of a 5 mg/mL MTT solution was applied and incubated for 4 h. Each well received 100 µL of dimethyl sulfoxide to dissolve the produced purple formazan. The colorimetric test was monitored and recorded at an absorbance of 570 nm via a plate reader (EXL 800, New York, NY, USA). The relative cell viability was calculated as (A570 of treated samples/A570 of untreated samples) × 100 and represented as a percentage.

3. Results

3.1. Characterization

X-ray Diffraction characteristics

The XRD analysis of the generated pure nano propolis, ZnO NPs, and ZnO-P NCs is shown in Figure 3. The pure nano propolis structure pattern can be seen in the region 2θ = 21.35°, according to the literature [60]. The XRD spectrum of ZnO NPs indicates the clear presence of synthesized ZnO NPs at 2θ = 33.4° and 37.1°, which coincides with the indexes of (002) and (101), respectively, depending on the JCPDS card No. (76-0704). The XRD spectrum of the nanocomposite ZnO-P NCs obtained distinctive patterns at 2θ = 21.9° and 34.4° that belonged to the nano propolis and zinc oxide, respectively. These patterns are a high signature for blending zinc oxide nanoparticles into the propolis structure.

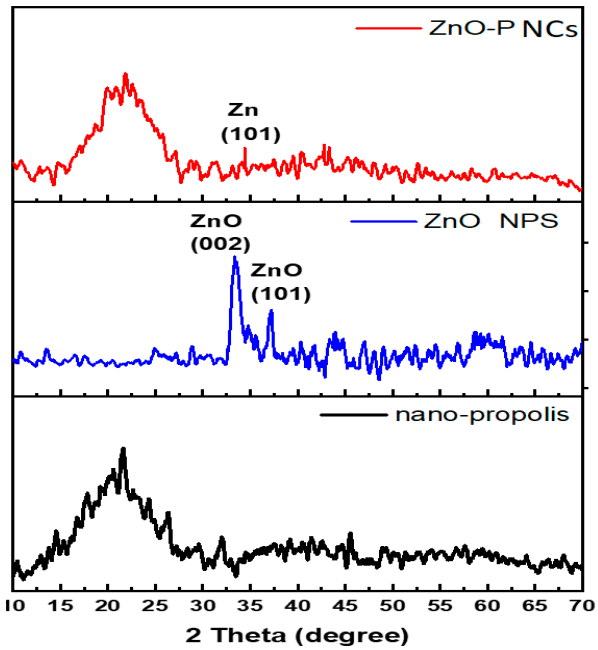

Figure 3. X-ray diffraction pattern of nano propolis, ZnO NPs, and ZnO-P NCs.

Using the Debye–Scherrer equation, the Zn-P NCs crystallite size (D) was calculated and is provided by the following equation [61].

$$D = K\lambda/\beta \cos\theta$$

wherein D is the size of the crystallite, K denotes the lattice constant, which was reported to be (0.94) in a homogeneous lattice and (0.89) in a heterogeneous one, λ indicates the X-ray's wavelength, CuKα indicates radiation (1.5406 Å), β denotes the full width at half maximum, and θ represents the incident angle. The nanocomposite's crystallite size was determined to be 9.70 nm at the peak's high intensity (2θ = 21.99°).

Fourier transforms infrared spectroscopy

Using an FTIR spectrophotometer, as shown in Figure 4, the functional groups within nano propolis and ZnO nanoparticles involved in synthesizing ZnO-P NCs were discovered. A shift was visible in the FTIR spectrum at a wavelength of 3371 cm^{-1}. The phenol functional group O-H and the stretching vibration of N-H in amides, both of which are often found in proteins, are supported by this result [62]. Additionally, the extract's inclusion of these functional groups aids in reducing zinc ions into zinc nanoparticles. Another study discovered that protein plays a role in reducing Zn^{2+} to ZnO [63]. Stretching vibrations of the C=C and C=O groups are shown by bands in the FTIR spectra of the propolis extract at 1631 cm^{-1} and = 1247.8 cm^{-1} [64]. Weak peaks in the 2925.4 cm^{-1} and 2854.18 cm^{-1} range indicate the presence of carbon in saturated hydrocarbons that are long-chain alkyl compounds. The absorptions in this region are typical aliphatic group (CH_2, CH_3) C-H bond vibrations [65]. Similar bands were also visible in the ZnO-P NCs FTIR spectra. In ZnO nanoparticle patterns, the stretching vibration of the hydroxyl (OH) groups causes prominent wide peaks in the upper area at 3140 cm^{-1} [66]. The C=O group is responsible for the peaks at 1558 cm^{-1} and at 1440 cm^{-1}. The –C–H bending vibration band appears [66]. The Zn-O bonds' stretching vibration, which is responsible for 688 and 454 cm^{-1}, validates this product's creation. As evidence that the synthesis process was successful in creating ZnO particles, the FTIR spectrum of ZnO-P NCs also exhibited bands between the wavelengths of 800 cm^{-1} and 450 cm^{-1}, denoting the vibrational strain absorption of the Zn-O bond (Table 1).

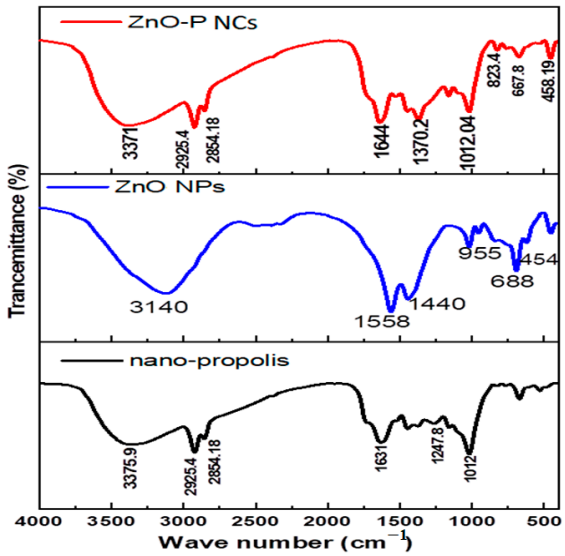

Figure 4. Characteristic FTIR spectrum of nano propolis, ZnO NPs, and ZnO-P NCs with assigned underlying molecular vibrations.

Table 1. Summary of the functional group's band position for the prepared materials.

Materials/Band Position (cm^{-1})			
Propolis	**ZnO**	**ZnO-P NCs**	**Characteristic Group**
3371	3140	3371	O-H and NH
2925.4		2925.4	CH_2
2854.18		2854.18	CH_3
1631		1644	C=C
1247.8	1558	1370.2	C=O
	1440		C-H
	688	667.8	Zn-O
	454	458.19	Zn-O

Scanning electron microscopy and transmission electron microscopy

The morphologies of as-prepared nano propolis, ZnO NPs, and ZnO-P NCs were characterized through SEM and TEM (Figure 5). Figure 5a shows the SEM images of propolis particles at 1 μm of magnification, displaying irregularly agglomerated particles, which are a few hundred nanometers in size. By contrast, SEM images of ZnO NPs (Figure 5b) at 200 nm magnification have spherical and smooth surface structures. Under the scale of 100 nm, ZnO-P NCs showed tiny spherical shapes with an approximately fair and uniform distribution without empty or cracked space on a large scale, as illustrated in Figure 5c. Furthermore, high-resolution TEM images of those three different samples demonstrate the ultrathin thickness structure of the nanosheets (Figure 5d). The spherical shape of ZnO NPs is clearly shown in Figure 5e, and they are distributed on the propolis sheet while tightly bonded together in ZnO-P NCs. The SEM observation (Figure 5f) is in accord with Figure 3, which indicates the crystallinity of the particles. Figure 5g indicates the particle distribution of ZnO-P NCs that range from 12 to 22 nm.

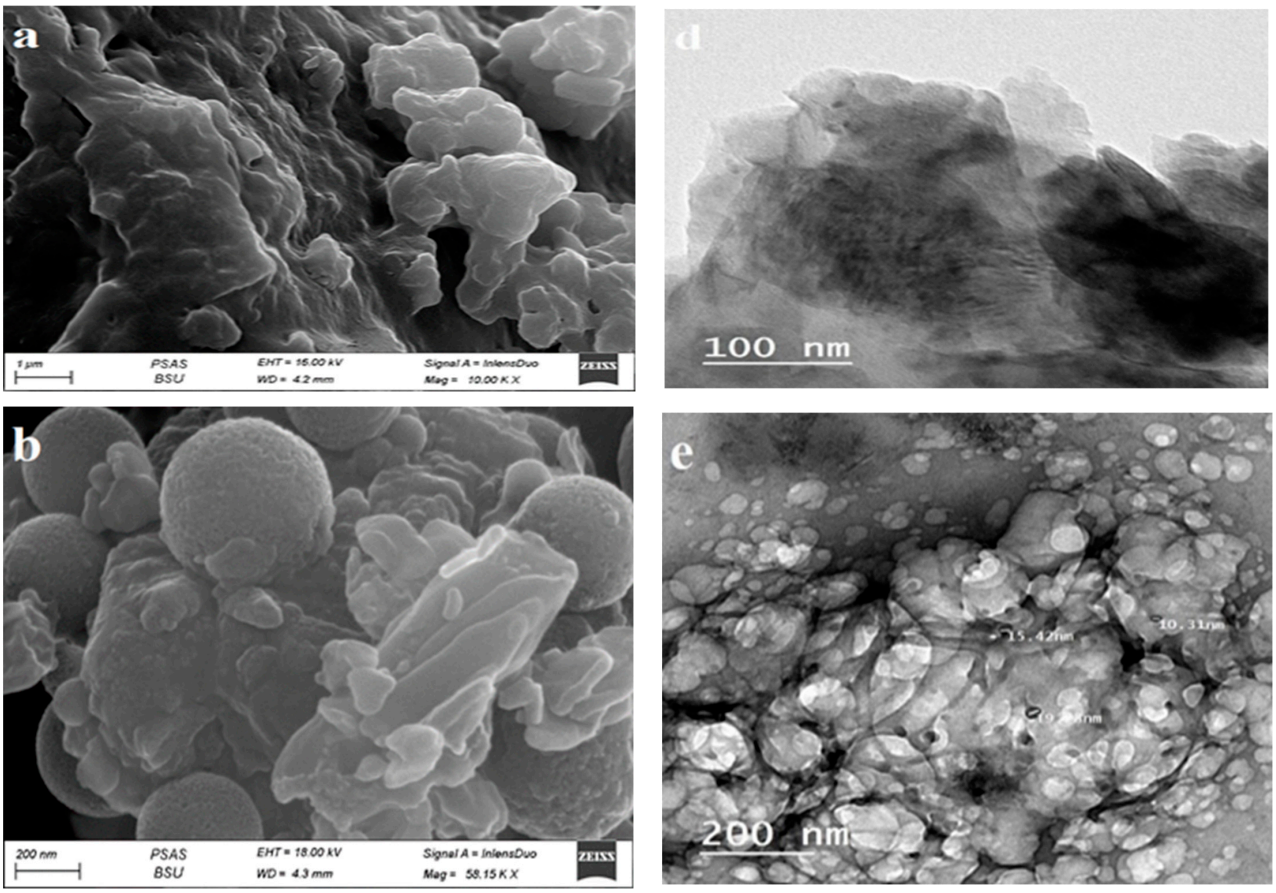

Figure 5. *Cont.*

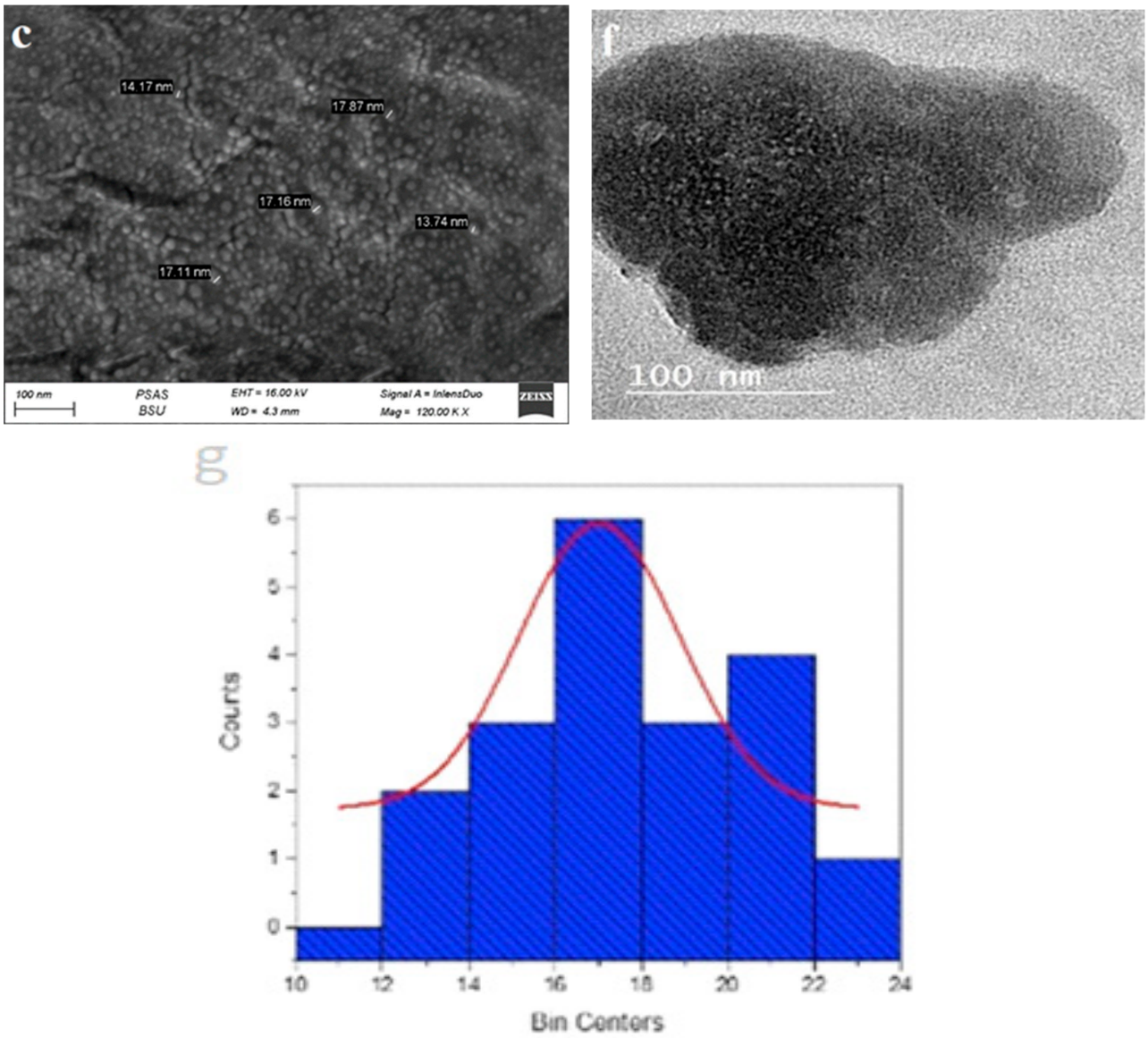

Figure 5. SEM of propolis (**a**), ZnO NPs (**b**), and ZnO-P NCs (**c**), TEM image of propolis (**d**), ZnO NPs (**e**), ZnO-P NCs (**f**) and particle size distribution of ZnO-P NCs (**g**).

Zeta potential

Zeta potential (ZP) values indicate the stability of the nanoparticles that have been synthesized. Thus, values of ZP between ±30 mV are considered optimal for good dispersion stabilization. According to Figure 6a–c, the nano propolis, ZnO NPs, and ZnO-P NCs had Zeta potential values of −34 mV, −11 mV, and −27 mV, respectively.

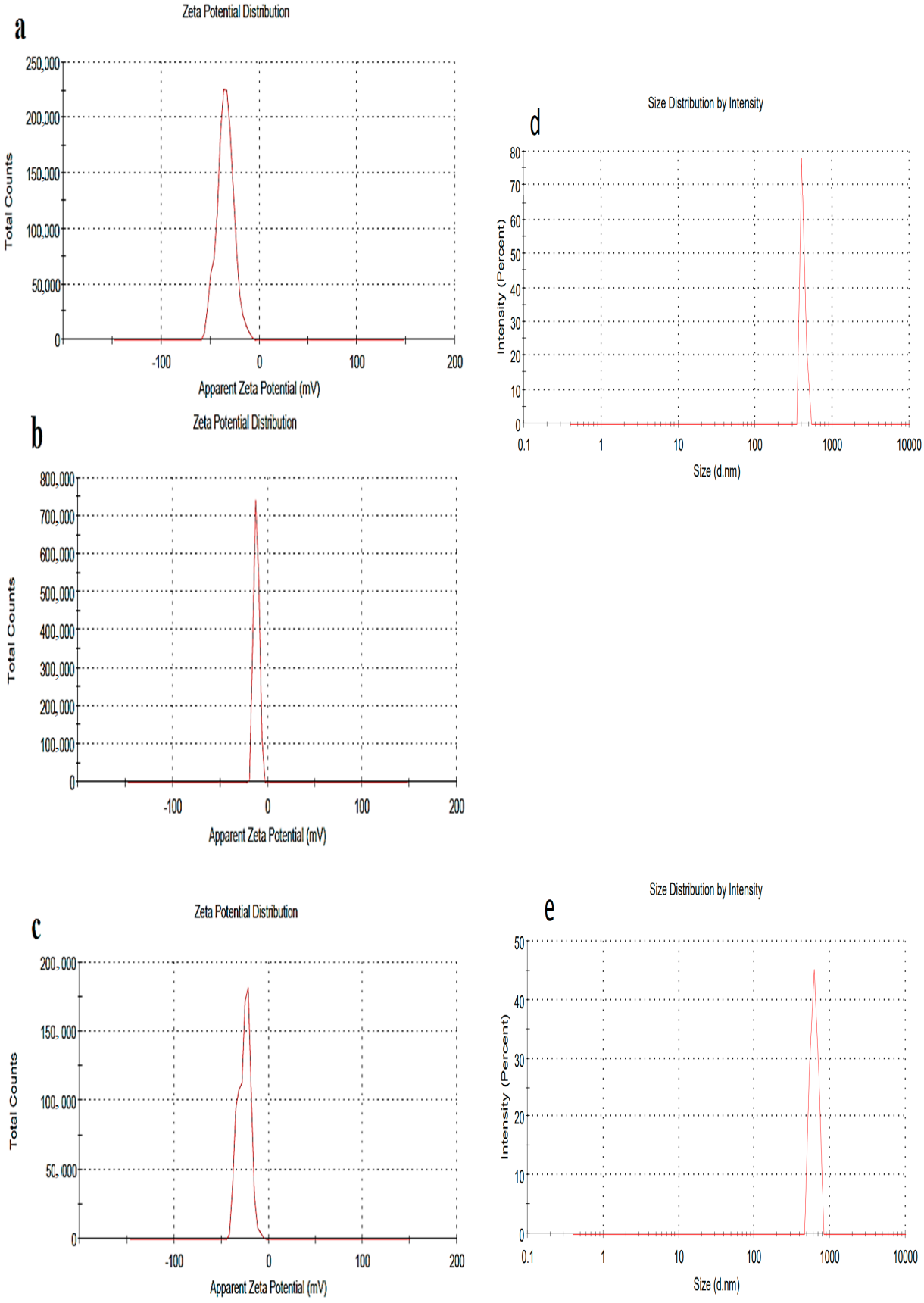

Figure 6. Zeta potential of nano propolis (**a**), ZnO NPs (**b**), and ZnO-P NCs(**c**), and DLS of ZnO NPs (**d**) and ZnO-P NCs (**e**).

DLS only offers information on the particles' average hydrodynamic diameter; TEM was used to decipher information on the interior characteristics of particles. Particle sizes smaller than that of 1601 and 1751 nm for ZnO NPs and ZnO-P NCs (Figure 6c,d), respectively, were visible in SEM and TEM pictures (Figure 5). This is because the largest particles produce the strongest scatters. DLS overestimates the relative contribution of these particles by measuring the intensity-weighted average particle size. Additionally, DLS measures colloids' equivalent hydrodynamic diameter, which is greater than the diameter seen in SEM and TEM. The value of the hydrodynamic size of the nanocomposite, more than that of Zn NPs, confirms the formation of the nanocomposite [67].

Optical properties

UV-vis absorption patterns were examined to learn more about the optical properties and energy structures of pure nano propolis, ZnO NPs, and the ZnO-P NCs, as shown in Figure 7. In Figure 7a, the UV-Vis spectrum includes distinctive absorbance peaks of pure nano propolis, ZnO NPs, and the ZnO-P NCs at roughly 273, 279, and 280 nm, respectively. For the ZnO-P NCs (blue), the absorption tended to produce an increase in higher wavelengths (280 nm), displaying the red shift [68]. Studies show that the wavelength increases as particle size increases, proving the formation of ZnO-P NCs. At high absorption regions, the optical bandgap of nano propolis, ZnO NPs, and the ZnO-P NCs has been demonstrated by employing the Tauc equation:

$$Ah\nu = B\,(h\nu - Eg)^{n}$$

The incident light energy is denoted by hν and given by the formula hν = 1240/L. B denotes the absorbance, Eg denotes the bandgap energy indicated by extrapolating the straight area of the curves between αhν and $(\alpha h\nu)_2$, and the n constant demonstrates the transition mode [69–71]. The results demonstrate that the bandgap energy of nano propolis, ZnO NPs, and ZnO-P NCs are 2.39 eV, 2.72 eV, and 3 eV, respectively.

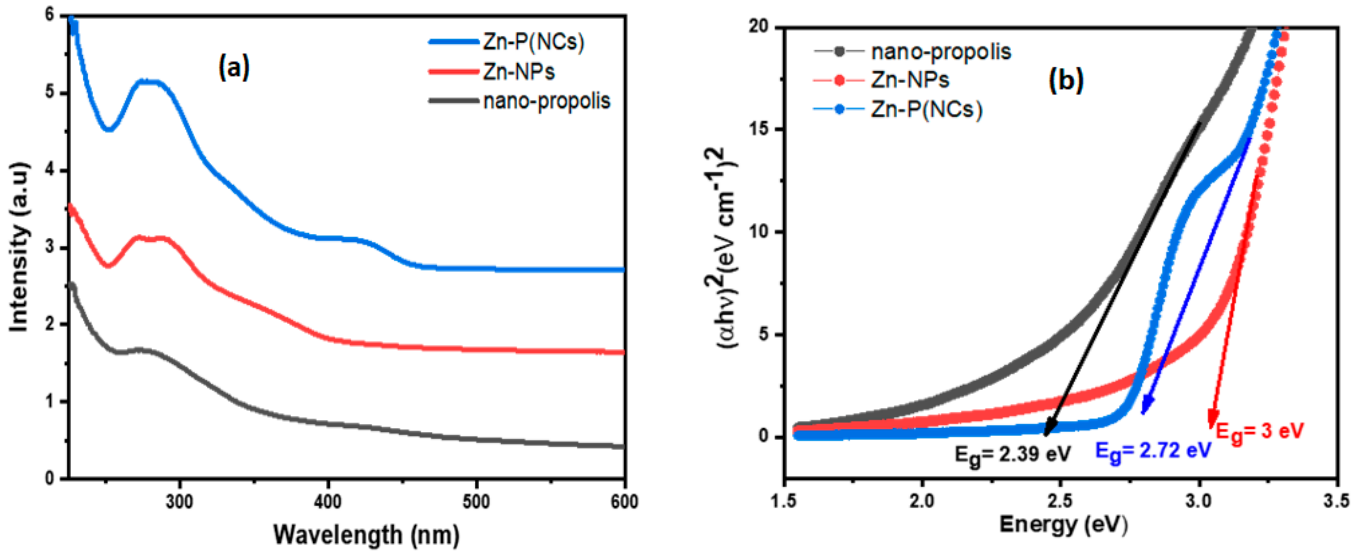

Figure 7. (**a**) UV-vis absorption spectra and (**b**) Bandgap of the nano propolis, ZnO NPs, and the ZnO–P NCs nanocomposite.

3.2. Biological Activities

Antioxidant activity

The antioxidant capabilities of propolis have been proven previously [72–76]. However, this work attempted to effectively enhance propolis' antioxidant activity by combining it with ZnO NPs in a final nanomaterial (nanocomposite). The DPPH assay was used to measure the free radicals scavenging activity of nano propolis, ZnO NPs, and the ZnO-P

NCs. Various concentrations were used, as shown in Figure 8, with an IC_{50} value of 2.75, 1.7, and 1.45 mg mL^{-1} for ZnO NPs, nano propolis, and ZnO-P NCs, respectively, and the evaluated nanomaterials demonstrated a high antioxidant DPPH radical scavenging activity in a dose-dependent manner.

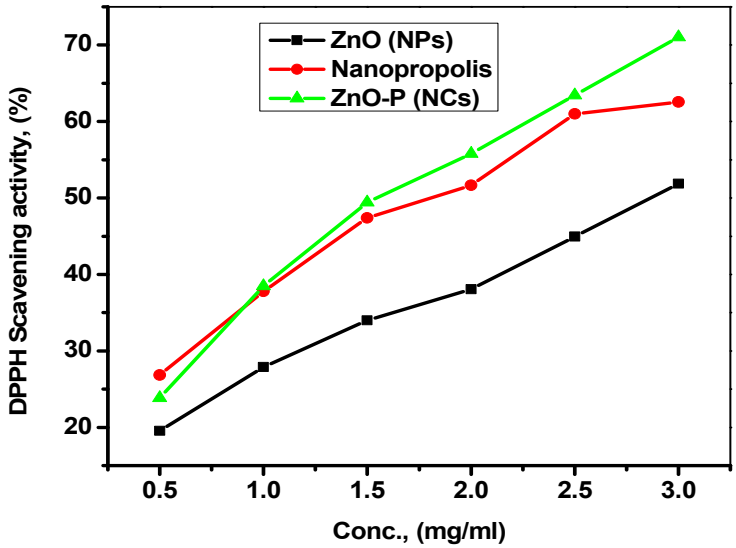

Figure 8. DPPH free radical scavenging activity of nano propolis, ZnO NPs and their composite.

Nano propolis and ZnO NPs both exhibited antioxidant capabilities that were effective in scavenging damaging free radicals and reducing oxidative stress. In green-synthesized ZnO-P NCs, antioxidant capacity was further enhanced through synergistic interactions. The bioactive compounds in propolis, such as flavonoids and phenolic acids, work with zinc oxide nanoparticles to scavenge free radicals more effectively, which could protect cells from oxidative damage and potentially alleviate oxidative stress-related conditions (Table 2).

Table 2. DPPH free radical scavenging activity of nano propolis, ZnO NPs, ZnO-P NCs, and their IC_{50} (mg mL^{-1}).

Sample	DPPH % Scavenging Activity	IC_{50} (mg mL^{-1})
Nano propolis	51.85	1.7
ZnO NPs	62.56	2.75
ZnO-P NCs	71.02	1.45

This study compares the antioxidant activity of propolis, ZnO nanoparticles, and their composites, highlighting several key aspects. Diverse composition: propolis contains various compounds contributing to its antioxidant potential, while ZnO nanoparticles offer unique antioxidant mechanisms. Emerging nanotechnology: this research explores the novel use of ZnO nanoparticles, offering insights into nanomaterials' advantages in combating oxidative stress. Synergistic effects: the synergistic effects are assessed when combining natural compounds with nanomaterials. These mechanisms complement each other, covering a broader spectrum of oxidative stressors. Nano propolis can directly scavenge free radicals, while ZnO NPs participate in redox reactions and neutralize ROS by donating or accepting electrons. They can enhance their overall capacity to neutralize various types of free radicals and oxidative species when used together. ZnO NPs improve the stability and bioavailability of active compounds in nano propolis. They act as carriers or delivery vehicles for nano propolis antioxidants, protecting them from degradation and ensuring a more sustained release of antioxidants. Some ZnO NPs exhibit catalytic activity, accelerating the breakdown of harmful oxidative species like hydrogen peroxide. This

amplifies propolis's antioxidant effect by increasing the rate at which ROS are eliminated. Safety and applications: evaluating safety profiles is crucial for various applications, from cosmetics to biomedical uses. Environmental considerations: this study assesses the environmental impact of these materials.

Cytotoxic activity

Propolis was reported to have potential antitumor properties using various mechanisms. In addition, ZnO NPs are considered a promising anticancer agent due to their unique biocompatibility properties, high selectivity, enhanced cytotoxicity, and ease of synthesis [77]. ZnO-P NCs have a higher activity than other samples. Hence, the in vitro cytotoxicity of synthesized nanomaterials was determined against breast cancer and cervical carcinoma (MCF-7 and Hela) via the MTT assay. In addition, a normal human cell line (WI-38) was utilized to assess the selectivity, and doxorubicin was chosen as a standard anticancer treatment for comparison (Table 3). A parallel line assay (PLA version 1.2.06) was used for statistical analysis, and both were discovered to be similarly cytotoxic and effective. The concentration that led to a 50% loss of the cell monolayer (IC_{50}) was used to measure cytotoxicity. The obtained results revealed that nano propolis, ZnO NPs, and their nanocomposite ZnO-P NCs could, in a dose-dependent manner, inhibit the proliferation of the selected cell lines (Figure 9).

Table 3. In vitro cytotoxic activities of nano propolis, ZnO NPs and ZnO-P NCs against human cell lines.

Compound	In Vitro Cytotoxicity IC_{50} (μg/mL)		
	WI38	**Hela**	**MCF7**
DOX	6.72 ± 0.5	5.57 ± 0.4	4.17 ± 0.2
Nano propolis	75.48 ± 3.9	49.01 ± 2.8	38.96 ± 2.3
ZnO NPs	43.10 ± 2.6	52.36 ± 3.0	68.80 ± 3.5
ZnO-P NCs	57.09 ± 3.3	23.77 ± 1.9	18.17 ± 1.4

Additionally, a more potent cytotoxic activity was observed for ZnO-P NCs (IC_{50} = 18.17 ± 1.4 μg/mL and 23.77 ± 1.9 μg/mL against MCF-7 and Hela cell lines, respectively. The significant difference in IC_{50} values confirmed its more effective ability to penetrate cells. Moreover, ZnO-P NCs showed higher selectivity toward tumor cells than the normal cell line (WI-38). They showed higher selectivity than the standard used (DOX). The results displayed in Figure 9 and Table 3 further support the selectivity of these novel compounds and indicate how their lower toxicity toward normal cells was also observed. The propolis nanocomposite is a perfect adjuvant agent for upcoming anticancer regimens due to its excellent outcomes, good oral bioavailability, and favorable historical safety profile [78,79].

It is important to note that the specific mechanisms underlying the synergy effect between zinc oxide nanoparticles and nano propolis in their composite formulation may vary depending on the preparation method, ratio, and concentration of the components. Furthermore, the observed synergy needs to be supported by rigorous scientific research and evaluation in preclinical and clinical studies to understand its extent and potential therapeutic applications fully.

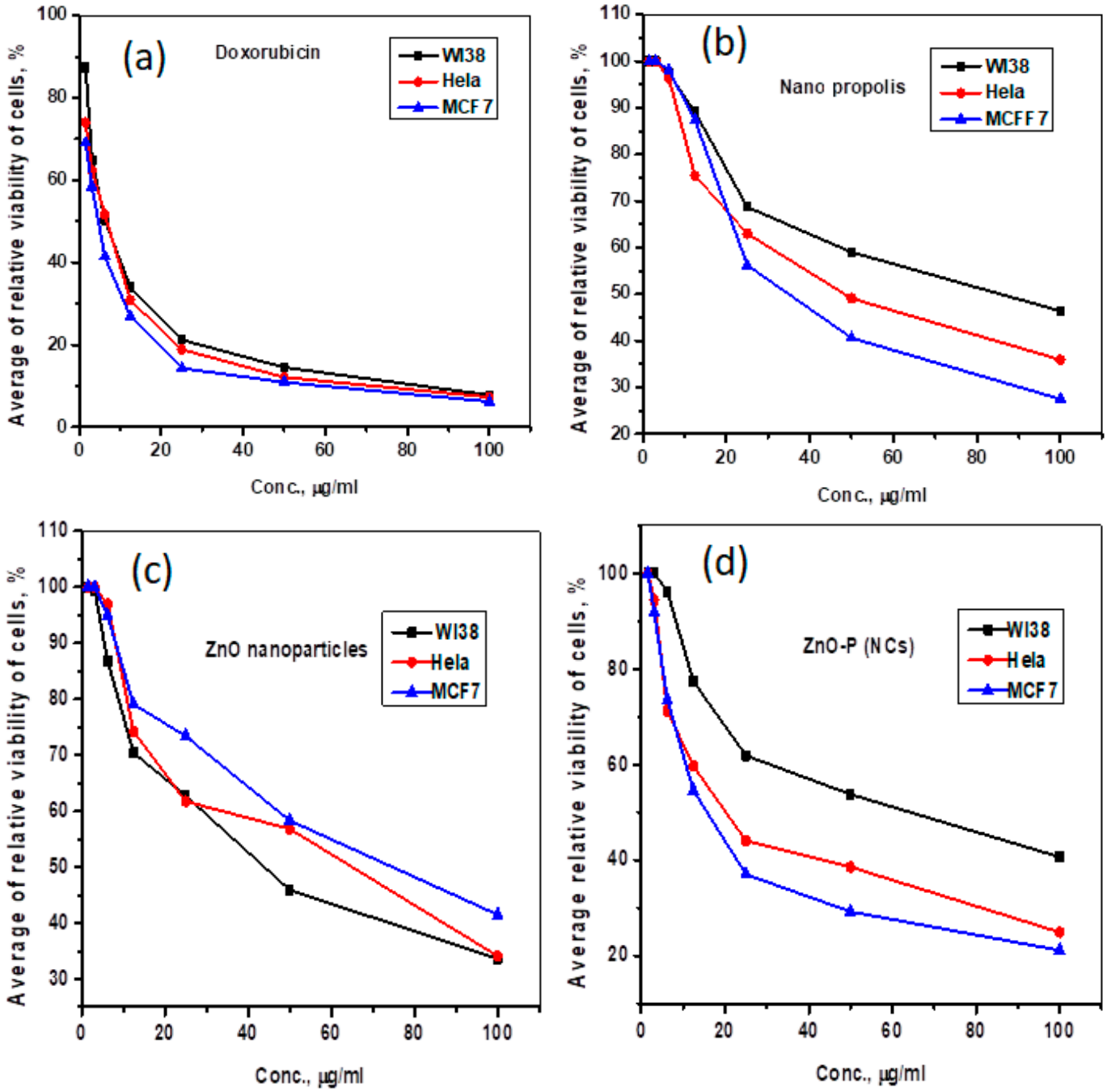

Figure 9. Average relative viability (%) of the lung fibroblast cell line (WI 38), human cervical cancer cell line (Hela), and breast carcinoma cell line (MCF7) at various concentrations of (**a**) doxorubicin, (**b**) nano propolis, (**c**) ZnO NPs and (**d**) ZnO-P NCs.

Comparison of the DPPH free radical scavenging activity

Our findings have been further evaluated in comparison to the values obtained with other metals and metal oxide nanoparticles (Table 4).

The data in Table 4 show that the DPPH scavenging activity of zinc oxide, propolis, and ZnO-P NCs has a significant value compared with other materials. However, these data confirm the dependency of antioxidant activity on concentration.

Table 4. Comparison of the DPPH free radical scavenging activity.

Sample	DPPH % Scavenging Activity	Ref.
Nano propolis	51.85	This work
ZnO NPs	62.56	This work
ZnO-P NCs	71.02	This work
Cellulose	4.29	[80]
ZnO NPs	6.75	[80]
ZnO-Cel	14.85	[80]
Rut-Zn	41.92	[81]
Cit-Zn	31.33	[81]
MgO NPs	43.16	[82]
Gold	50	[83]
Silver	55	[83]
Copper oxide	85 (Conc. = 37.5 mg/mL)	[84]
Nickel oxide	90 (Conc. = 33.3 mg/mL)	[85]

4. Conclusions

Propolis NPs were prepared, and their extract was used to obtain ZnO NPs and ZnO-P NCs using a biomimetic, environmentally friendly, simple, and cost-effective approach compared to other reported methods. The nanomaterials were characterized using Zeta potential analysis, FT-IR, XRD, SEM, and TEM. The results confirm the formation and stability of nanomaterials, and the particle size of ZnO-P NC was 9.70 ± 0.03 nm.

Propolis contains bioactive compounds such as flavonoids, phenolic acids, and terpenoids, contributing to its potent antioxidant and anticancer effects. Its ability to inhibit cancer cell proliferation, induce cell cycle arrest, and promote cancer cell death is attributed to its antioxidant properties, protecting cells from oxidative damage and reducing cancer risk. The synthesized nanomaterials were evaluated for their antioxidant activity, showing promising DPPH radical scavenging effects with IC50 values of 2.75, 1.7, and 1.45 mg mL^{-1} for ZnO NPs, propolis NPs, and ZnO PNCs, respectively. Furthermore, the anticancer activity of ZnO PNCs was investigated on breast cancer (Hela and MCF-7) and human normal (W138) cell lines. The ZnO PNCs exhibited potent cytotoxicity against breast cancer cells, with an IC_{50} value of 18 μg/mL, suggesting its potential for breast cancer treatment. It also displayed anticancer effects against cervical cancer with an IC50 value of 23 μg/mL. The synergy between zinc oxide nanoparticles and nano propolis in their composite formulation contributed to its observed safety, antioxidant, and anticancer activities.

This study shows promising results, including in vivo experiments and clinical trials, while highlighting the potential of natural compounds and nanotechnology in developing novel therapeutic strategies to combat oxidative stress-related disorders and cancer. However, further research is needed for comprehensive evaluation and potential applications.

Author Contributions: Conceptualization, R.R.A. and R.M.; methodology, R.R.A. and R.M.; software, R.R.A., D.E., S.A.S. and S.A.-E.; validation, R.R.A. and R.M.; formal analysis, R.R.A., S.A.S. and R.M.; investigation, S.A.S., D.E. and E.M.K.; resources, R.R.A., A.A.F., Y.F.A. and R.M.; data curation, R.R.A. and R.M.; writing—original draft preparation, R.R.A. and S.A.S.; writing—review and editing, R.R.A.; visualization, R.R.A.; supervision, R.R.A. and R.M.; project administration, D.H.M.A., W.N.H. and R.M.; funding acquisition, R.M. All authors have read and agreed to the published version of the manuscript.

Funding: This research was funded by grants from the Princess Nourah bint Abdulrahman University Researchers Supporting Project (grant number, PNURSP2023R15), Princess Nourah bint Abdulrahman University, Riyadh, Saudi Arabia.

Data Availability Statement: All relevant data used to produce these results are entirely available from the corresponding author on reasonable request.

Acknowledgments: The authors acknowledge Princess Nourah bint Abdulrahman University Researchers Supporting Project number (PNURSP2023R15), Princess Nourah bint Abdulrahman University, Riyadh, Saudi Arabia.

Conflicts of Interest: The authors declare no conflict of interest.

References

1. Luechinger, N.A.; Grass, R.N.; Athanassiou, E.K.; Stark, W.J. Bottom-up fabrication of metal/metal nanocomposites from nanoparticles of immiscible metals. *Chem. Mater.* **2010**, *22*, 155–160. [CrossRef]
2. Liu, J.; Qiao, S.Z.; Hu, Q.H.; Max Lu, G.Q. Magnetic Nanocomposites: Magnetic Nanocomposites with Mesoporous Structures: Synthesis and Applications (Small 4/2011). *Small* **2011**, *7*, 418. [CrossRef]
3. Prabhu, S.; Poulose, E.K. Silver nanoparticles: Mechanism of antimicrobial action, synthesis, medical applications, and toxicity effects. *Int. Nano Lett.* **2012**, *2*, 32. [CrossRef]
4. Sudheer, S.; Bai, R.G.; Muthoosamy, K.; Tuvikene, R.; Gupta, V.K.; Manickam, S. Biosustainable production of nanoparticles via mycogenesis for biotechnological applications: A critical review. *Environ. Res.* **2022**, *204*, 111963. [CrossRef]
5. Singh, J.; Dutta, T.; Kim, K.H.; Rawat, M.; Samddar, P.; Kumar, P. "Green" synthesis of metals and their oxide nanoparticles: Applications for environmental remediation. *J. Nanobiotechnol.* **2018**, *16*, 84. [CrossRef]
6. Andhari, S.S.; Wavhale, R.D.; Dhobale, K.D.; Tawade, B.V.; Chate, G.P.; Patil, Y.N.; Khandare, J.J.; Banerjee, S.S. Self-Propelling Targeted Magneto-Nanobots for Deep Tumor Penetration and pH-Responsive Intracellular Drug Delivery. *Sci. Rep.* **2020**, *10*, 4703. [CrossRef]
7. Mittal, A.K.; Chisti, Y.; Banerjee, U.C. Synthesis of metallic nanoparticles using plant extracts. *Biotechnol. Adv.* **2013**, *31*, 346–356. [CrossRef]
8. Surek, M.; Fachi, M.M.; de Fátima Cobre, A.; de Oliveira, F.F.; Pontarolo, R.; Crisma, A.R.; de Souza, W.M.; Felipe, K.B. Chemical composition, cytotoxicity, and antibacterial activity of propolis from Africanized honeybees and three different Meliponini species. *J. Ethnopharmacol.* **2021**, *269*, 113662. [CrossRef]
9. Kolaylı, S.; Birinci, C.; Kara, Y.; Ozkok, A.; Samancı, A.E.T.; Sahin, H.; Yildiz, O. A melissopalynological and chemical characterization of Anatolian propolis and an assessment of its antioxidant potential. *Eur. Food Res. Technol.* **2023**, *249*, 1213–1233. [CrossRef]
10. Rocha, V.M.; Portela, R.D.; dos Anjos, J.P.; de Souza, C.O.; Umsza-Guez, M.A. Stingless bee propolis: Composition, biological activities and its applications in the food industry. *Food Prod. Process. Nutr.* **2023**, *5*, 29. [CrossRef]
11. Ngaini, Z.; Hussain, H.; Kelabo, E.S.; Wahi, R.; Farooq, S. Chemical profiling, biological properties and environmental contaminants of stingless bee honey and propolis. *J. Apic. Res.* **2023**, *62*, 131–147. [CrossRef]
12. Berretta, A.A.; Zamarrenho, L.G.; Correa, J.A.; De Lima, J.A.; Borini, G.B.; Ambrósio, S.R.; Barud, H.d.S.; Bastos, J.K.; De Jong, D. Development and Characterization of New Green Propolis Extract Formulations as Promising Candidates to Substitute for Green Propolis Hydroalcoholic Extract. *Molecules* **2023**, *28*, 3510. [CrossRef] [PubMed]
13. Lotfy, M. Biological activity of bee propolis in health and disease. *Asian Pacific J. Cancer Prev.* **2006**, *7*, 22–31.
14. Marcucci, M.C. Propolis: Chemical composition, biological properties and therapeutic activity. *Apidologie* **1995**, *26*, 83–99. [CrossRef]
15. Braakhuis, A. Evidence on the health benefits of supplemental propolis. *Nutrients* **2019**, *11*, 2705. [CrossRef]
16. Bankova, V.; Boudourova-Krasteva, G.; Frete, X.; Popov, S.; Sforcin, J.M.; Maimoni-Rodella, R.; Kujumgiev, A. Phytochemical Evidence for the Plant Origin of Brazilian Propolis from São Paulo State. *Z. Fur Naturforsch.—Sect. C J. Biosci.* **1999**, *54*, 401–405. [CrossRef]
17. Sforcin, J.M.; Bankova, V. Propolis: Is there a potential for the development of new drugs? *J. Ethnopharmacol.* **2011**, *133*, 253–260. [CrossRef]
18. Burdock, G.A. Review of the biological properties and toxicity of bee propolis (propolis). *Food Chem. Toxicol.* **1998**, *36*, 347–363. [CrossRef]
19. Shahidi, F.; Ambigaipalan, P. Phenolics and polyphenolics in foods, beverages and spices: Antioxidant activity and health effects—A review. *J. Funct. Foods* **2015**, *18*, 820–897. [CrossRef]
20. Wang, W.; Xiong, P.; Zhang, H.; Zhu, Q.; Liao, C.; Jiang, G. Analysis, occurrence, toxicity and environmental health risks of synthetic phenolic antioxidants: A review. *Environ. Res.* **2021**, *201*, 111531. [CrossRef]
21. Bonamigo, T.; Campos, J.F.; Alfredo, T.M.; Balestieri, J.B.P.; Cardoso, C.A.L.; Paredes-Gamero, E.J.; De Picoli Souza, K.; Dos Santos, E.L. Antioxidant, Cytotoxic, and Toxic Activities of Propolis from Two Native Bees in Brazil: Scaptotrigona depilis and Melipona quadrifasciata anthidioides. *Oxid. Med. Cell. Longev.* **2017**, *2017*, 1038153. [CrossRef] [PubMed]
22. Fabris, S.; Bertelle, M.; Astafyeva, O.; Gregoris, E.; Zangrando, R.; Gambaro, A.; Lima, G.P.P.; Stevanato, R. Antioxidant Properties and Chemical Composition Relationship of Europeans and Brazilians Propolis. *Pharmacol. Pharm.* **2013**, *4*, 46–51. [CrossRef]
23. Xuan, H.; Li, Z.; Yan, H.; Sang, Q.; Wang, K.; He, Q.; Wang, Y.; Hu, F. Antitumor activity of Chinese propolis in human breast cancer MCF-7 and MDA-MB-231 cells. *Evid.-Based Complement. Altern. Med.* **2014**, *2014*, 280120. [CrossRef] [PubMed]
24. Singla, S.; Kumar, N.; Kaur, J. In vivo studies on the protective effect of propolis on doxorubicin-induced toxicity in liver of male rats. *Toxicol. Int.* **2014**, *21*, 191. [CrossRef] [PubMed]

25. Salem, M.M.; Donia, T.; Abu-Khudir, R.; Ramadan, H.; Ali, E.M.M.; Mohamed, T.M. Propolis Potentiates Methotrexate Anticancer Mechanism and Reduces its Toxic Effects. *Nutr. Cancer* **2020**, *72*, 460–480. [CrossRef] [PubMed]
26. Benguedouar, L.; Lahouel, M.; Gangloff, S.; Durlach, A.; Grange, F.; Bernard, P.; Antonicelli, F. Algerian ethanolic extract of Propolis and galangin decreased melanoma tumour progression in C57BL6 mice. *Ann. Dermatol. Venereol.* **2015**, *142*, S294. [CrossRef]
27. Demir, S.; Aliyazicioglu, Y.; Turan, I.; Misir, S.; Mentese, A.; Yaman, S.O.; Akbulut, K.; Kilinc, K.; Deger, O. Antiproliferative and proapoptotic activity of Turkish propolis on human lung cancer cell line. *Nutr. Cancer* **2016**, *68*, 165–172. [CrossRef]
28. Rouibah, H.; Kebsa, W.; Lahouel, M.; Zihlif, M.; Ahram, M.; Aburmaileh, B.; Mansour Al Shhab, M.A.; Al-Ameer, H.J.; Mustafa, E. Algerian propolis: Between protection of normal cells and potentialisation of the anticancer effects of doxorubicin against breast cancer cells via P-glycoprotein inhibition and cell cycle arrest in the S phase. *J. Physiol. Pharmacol.* **2021**, *72*, 2. [CrossRef]
29. Diva, A.N.; Pratami, D.K.; Wijanarko, A.; Hermansyah, H.; Sahlan, M. Effect of ethanolic propolis extract from *Tetragonula biroi* bees on the growth of human cancer cell lines HeLa and MCF-7. In *3RD BIOMEDICAL ENGINEERING'S RECENT PROGRESS IN BIOMATERIALS, DRUGS DEVELOPMENT, AND MEDICAL DEVICES, Proceedings of the International Symposium of Biomedical Engineering (ISBE) 2018, Jakarta, Indonesia, 6–8 August 2018*; AIP Conference Proceedings; AIP (ACP): College Park, MD, USA, 2019.
30. Turan, I.; Demir, S.; Misir, S.; Kilinc, K.; Mentese, A.; Aliyazicioglu, Y.; Deger, O. Cytotoxic effect of Turkish propolis on liver, colon, breast, cervix and prostate cancer cell lines. *Trop. J. Pharm. Res.* **2015**, *14*, 777. [CrossRef]
31. Forma, E.; Bryś, M. Anticancer activity of propolis and its compounds. *Nutrients* **2021**, *13*, 2594. [CrossRef]
32. Javed, S.; Mangla, B.; Ahsan, W. From propolis to nanopropolis: An exemplary journey and a paradigm shift of a resinous substance produced by bees. *Phyther. Res.* **2022**, *36*, 2016–2041. [CrossRef] [PubMed]
33. Thakkar, S.; Sharma, D.; Kalia, K.; Tekade, R.K. Tumor microenvironment targeted nanotherapeutics for cancer therapy and diagnosis: A review. *Acta Biomater.* **2020**, *101*, 43–68. [CrossRef] [PubMed]
34. Zheng, Y.; Li, Z.; Chen, H.; Gao, Y. Nanoparticle-based drug delivery systems for controllable photodynamic cancer therapy. *Eur. J. Pharm. Sci.* **2020**, *144*, 105213. [CrossRef] [PubMed]
35. Mirzaei, H.; Darroudi, M. Zinc oxide nanoparticles: Biological synthesis and biomedical applications. *Ceram. Int.* **2017**, *43*, 907–914. [CrossRef]
36. Singh, T.A.; Sharma, A.; Tejwan, N.; Ghosh, N.; Das, J.; Sil, P.C. A state of the art review on the synthesis, antibacterial, antioxidant, antidiabetic and tissue regeneration activities of zinc oxide nanoparticles. *Adv. Colloid Interface Sci.* **2021**, *295*, 102495. [CrossRef]
37. Hermansyah, D.; Zulhendri, F.; Perera, C.O.; Firsty, N.N.; Chandrasekaran, K.; Abdulah, R.; Herman, H.; Lesmana, R. The Potential Use of Propolis as an Adjunctive Therapy in Breast Cancers. *Integr. Cancer Ther.* **2022**, *21*, 15347354221096868. [CrossRef]
38. Rasmussen, J.W.; Martinez, E.; Louka, P.; Wingett, D.G. Zinc oxide nanoparticles for selective destruction of tumor cells and potential for drug delivery applications. *Expert Opin. Drug Deliv.* **2010**, *7*, 1063–1077. [CrossRef]
39. Katwal, G.; Paulose, M.; Rusakova, I.A.; Martinez, J.E.; Varghese, O.K. Rapid Growth of Zinc Oxide Nanotube-Nanowire Hybrid Architectures and Their Use in Breast Cancer-Related Volatile Organics Detection. *Nano Lett.* **2016**, *16*, 3014–3021. [CrossRef]
40. Firdous, S. Development and imaging of zinc oxide nanorods as a photosensitizer for the diagnosis and treatment of cancer using lasers. *Laser Phys. Lett.* **2018**, *15*, 095604. [CrossRef]
41. Hatami, R.; Javadi, A.; Jafarizadeh-Malmiri, H. Effectiveness of six different methods in green synthesis of selenium nanoparticles using propolis extract: Screening and characterization. *Green Process. Synth.* **2020**, *9*, 685–692. [CrossRef]
42. Bankova, V.S.; De Castro, S.L.; Marcucci, M.C. Propolis: Recent advances in chemistry and plant origin. *Apidologie* **2000**, *31*, 3–15. [CrossRef]
43. Hajizadeh, Y.S.; Harzandi, N.; Babapour, E.; Yazdanian, M.; Ranjbar, R. Green Synthesize and Characterization of Copper Nanoparticles Using Iranian Propolis Extracts. *Adv. Mater. Sci. Eng.* **2022**, *2022*, 8100440. [CrossRef]
44. Priyadarshini, J.F.; Sivakumari, K.; Selvaraj, R.; Ashok, K.; Jayaprakash, P.; Rajesh, S. Green synthesis of silver nanoparticles from propolis. *Res. J. Life Sci. Bioinform. Pharm. Chem. Sci.* **2018**, *4*, 23–36.
45. Barsola, B.; Kumari, P. Green synthesis of nano-propolis and nanoparticles (Se and Ag) from ethanolic extract of propolis, their biochemical characterization: A review. *Green Process. Synth.* **2022**, *11*, 659–673. [CrossRef]
46. Bayrami, M.; Bayrami, A.; Habibi-Yangjeh, A.; Shafeeyan, M.S.; Feizpoor, S.; Arvanagh, F.M.; Nourani, M.R.; Taheri, R.A. Biologically-synthesised ZnO/CuO/Ag nanocomposite using propolis extract and coated on the gauze for wound healing applications. *IET Nanobiotechnol.* **2020**, *14*, 548–554. [CrossRef]
47. Li, W.; Zhao, D.; Li, W.; Wen, R.; Liu, X.; Liu, L.; Li, T.; Fan, L. Chemorobust dye-encapsulated framework as dual-emission self-calibrating ratiometric sensor for intelligent detection of toluene exposure biomarker in urine. *Spectrochim. Acta—Part A Mol. Biomol. Spectrosc.* **2023**, *296*, 122637. [CrossRef]
48. Wang, F.; Zhao, D.; Li, W.; Zhang, H.; Li, B.; Hu, T.; Fan, L. Rod-shaped units based cobalt(II) organic framework as an efficient electrochemical sensor for uric acid detection in serum. *Microchem. J.* **2023**, *185*, 108154. [CrossRef]
49. Yin, J.; Li, W.; Li, W.; Liu, L.; Zhao, D.; Liu, X.; Hu, T.; Fan, L. Heterometallic ZnHoMOF as a Dual-Responsive Luminescence Sensor for Efficient Detection of Hippuric Acid Biomarker and Nitrofuran Antibiotics. *Molecules* **2023**, *28*, 6274. [CrossRef]
50. Zhao, D.; Li, W.; Wen, R.; Lei, N.; Li, W.; Liu, X.; Zhang, X.; Fan, L. Eu(III)-Functionalized MOF-Based Dual-Emission Ratiometric Sensor Integrated with Logic Gate Operation for Efficient Detection of Hippuric Acid in Urine and Serum. *Inorg. Chem.* **2023**, *62*, 2715–2725. [CrossRef]

51. Rezk, N.; Abdelsattar, A.S.; Makky, S.; Hussein, A.H.; Kamel, A.G.; El-Shibiny, A. New formula of the green synthesised Au@Ag core@shell nanoparticles using propolis extract presented high antibacterial and anticancer activity. *AMB Express* **2022**, *12*, 108. [CrossRef]
52. Roy, S.; Priyadarshi, R.; Rhim, J.W. Development of multifunctional pullulan/chitosan-based composite films reinforced with ZnO nanoparticles and propolis for meat packaging applications. *Foods* **2021**, *10*, 2789. [CrossRef]
53. Mocanu, A.; Isopencu, G.; Busuioc, C.; Popa, O.M.; Dietrich, P.; Socaciu-Siebert, L. Bacterial cellulose films with ZnO nanoparticles and propolis extracts: Synergistic antimicrobial effect. *Sci. Rep.* **2019**, *9*, 17687. [CrossRef]
54. Matei, P.M.; Martín-Ramos, P.; Sánchez-Báscones, M.; Hernández-Navarro, S.; Correa-Guimaraes, A.; Navas-Gracia, L.M.; Rufino, C.A.; Ramos-Sánchez, M.C.; Martín-Gil, J. Synthesis of chitosan oligomers/propolis/silver nanoparticles composite systems and study of their activity against diplodia seriata. *Int. J. Polym. Sci.* **2015**, *2015*, 864729. [CrossRef]
55. Singh, R.P.; Shukla, V.K.; Yadav, R.S.; Sharma, P.K.; Singh, P.K.; Pandey, A.C. Biological approach of zinc oxide nanoparticles formation and its characterization. *Adv. Mater. Lett.* **2011**, *2*, 313–317. [CrossRef]
56. Moaty, S.A.A.; Farghali, A.A.; Khaled, R. Preparation, characterization and antimicrobial applications of Zn-Fe LDH against MRSA. *Mater. Sci. Eng. C* **2016**, *68*, 184–193. [CrossRef]
57. Meda, A.; Lamien, C.E.; Romito, M.; Millogo, J.; Nacoulma, O.G. Determination of the total phenolic, flavonoid and proline contents in Burkina Fasan honey, as well as their radical scavenging activity. *Food Chem.* **2005**, *91*, 571–577. [CrossRef]
58. Chang, C.C.; Yang, M.H.; Wen, H.M.; Chern, J.C. Estimation of total flavonoid content in propolis by two complementary colometric methods. *J. Food Drug Anal.* **2002**, *10*, 3. [CrossRef]
59. Hu, C.; Yuan, Y.V.; Kitts, D.D. Antioxidant activities of the flaxseed lignan secoisolariciresinol diglucoside, its aglycone secoisolariciresinol and the mammalian lignans enterodiol and enterolactone in vitro. *Food Chem. Toxicol.* **2007**, *45*, 2219–2227. [CrossRef]
60. Fidrianny, I.; Harnovi, M.; Insanu, M. Evaluation of antioxidant activities from various extracts of sweet orange peels using DPPH, FRAP assays and correlation with phenolic, flavonoid, carotenoid content. *Asian J. Pharm. Clin. Res.* **2014**, *7*, 186–190.
61. Maharani, A.; Rini, R.; Sugiman, S. Pengaruh Penggunaan Media Interaktif Animasi Terhadap Minat Belajar Matematika Peserta Didik. *Pedagog. J. Pendidik. Dasar* **2019**, *6*.
62. Fakhari, S.; Jamzad, M.; Kabiri Fard, H. Green synthesis of zinc oxide nanoparticles: A comparison. *Green Chem. Lett. Rev.* **2019**, *12*, 19–24. [CrossRef]
63. PD, D.A.; Plashintania, D.R.; Putri, R.M.; Wibowo, I.; Ramli, Y.; Herdianto, S.; Indarto, A. Synthesis of zinc oxide nanoparticles using methanol propolis extract (Pro-ZnO NPs) as antidiabetic and antioxidant. *PLoS ONE* **2023**, *18*, e0289125. [CrossRef]
64. Hilo, D.H.; Al-garawi, Z.S.; Ismail, A.H. Green synthesis of ZnO NPs using ginger extract and assessment of their antioxidant activity. *Egypt. J. Chem.* **2023**, *66*, 111–117. [CrossRef]
65. Corciovă, A.C.; Mircea, C.; Burlec, A.; Cioancă, O.C.; Tuchiluş, C.T.; Fifere, A.; Lungoci, A.; Lungoci, A.L.; Marangoci, N.; Hăncianu, M. Antioxidant, Antimicrobial and Photocatalytic Activities of Silver Nanoparticles Obtained by Bee Propolis Extract Assisted Biosynthesis. *Farmacia* **2019**, *67*, 482–489. [CrossRef]
66. Zin, N.B.M.; Azemin, A.; Rodi, M.M.M.; Rashid, Z.M.; Mohd, K.S. Application of FTIR fingerprints coupled with chemometric for comparison of stingless bee propolis from different extraction methods. *Malays. J. Fundam. Appl. Sci.* **2019**, *15*, 350–355. [CrossRef]
67. Svečnjak, L.; Marijanović, Z.; Okińczyc, P.; Kuś, P.M.; Jerković, I. Mediterranean propolis from the adriatic sea islands as a source of natural antioxidants: Comprehensive chemical biodiversity determined by GC-MS, ftiratr, UHPLC-DAD-QQTOF-MS, DPPH and FRAP assay. *Antioxidants* **2020**, *9*, 337. [CrossRef]
68. Mahalakshmi, S.; Hema, N.; Vijaya, P.P. In Vitro Biocompatibility and Antimicrobial activities of Zinc Oxide Nanoparticles (ZnO NPs) Prepared by Chemical and Green Synthetic Route—A Comparative Study. *BioNanoScience* **2019**, *10*, 112–121.
69. Mahmoud, R.; Moaty, S.A.; Mohamed, F.; Farghali, A. Comparative Study of Single and Multiple Pollutants System Using Ti-Fe Chitosan LDH Adsorbent with High Performance in Wastewater Treatment. *J. Chem. Eng. Data* **2017**, *62*, 3703–3722. [CrossRef]
70. Yousaf, S.; Zulfiqar, S.; Shahi, M.N.; Warsi, M.F.; Al-Khalli, N.F.; Aly Aboud, M.F.; Shakir, I. Tuning the structural, optical and electrical properties of NiO nanoparticles prepared by wet chemical route. *Ceram. Int.* **2020**, *46*, 3750–3758. [CrossRef]
71. Gupta, K.; Jana, P.C.; Meikap, A.K. Optical and electrical transport properties of polyaniline-silver nanocomposite. *Synth. Met.* **2010**, *160*, 1566–1573. [CrossRef]
72. Atta, A.; Abdelhamied, M.M.; Abdelreheem, A.M.; Berber, M.R. Flexible methyl cellulose/polyaniline/silver composite films with enhanced linear and nonlinear optical properties. *Polymers* **2021**, *13*, 1225. [CrossRef]
73. Mosnáčková, K.; Chehimi, M.M.; Fedorko, P.; Omastová, M. Polyamide grafted with polypyrrole: Formation, properties, and stability. *Chem. Pap.* **2013**, *67*, 979–994. [CrossRef]
74. Moţ, A.C.; Silaghi-Dumitrescu, R.; Sârbu, C. Rapid and effective evaluation of the antioxidant capacity of propolis extracts using DPPH bleaching kinetic profiles, FT-IR and UV-vis spectroscopic data. *J. Food Compos. Anal.* **2011**, *24*, 516–522. [CrossRef]
75. Hegazi, A.G.; Abd El Hady, F.K. Egyptian propolis: 3. Antioxidant, antimicrobial activities and chemical composition of propolis from reclaimed lands. *Z. Fur Naturforsch.—Sect. C J. Biosci.* **2002**, *57*, 395–402. [CrossRef]
76. Shehata, M.G.; Ahmad, F.T.; Badr, A.N.; Masry, S.H.; El-Sohaimy, S.A. Chemical analysis, antioxidant, cytotoxic and antimicrobial properties of propolis from different geographic regions. *Ann. Agric. Sci.* **2020**, *65*, 209–217. [CrossRef]
77. Kumazawa, S.; Hamasaka, T.; Nakayama, T. Antioxidant activity of propolis of various geographic origins. *Food Chem.* **2004**, *84*, 329–339. [CrossRef]

78. El Sohaimy, S.; Masry, S. Phenolic Content, Antioxidant and Antimicrobial Activities of Egyptian and Chinese Propolis. *Am. Eurasian J. Agric. Environ. Sci.* **2014**, *14*, 1116–1124. [CrossRef]
79. Bisht, G.; Rayamajhi, S. ZnO Nanoparticles: A Promising Anticancer Agent. *Nanobiomedicine* **2016**, *3*, 9. [CrossRef]
80. Patel, S. Emerging Adjuvant Therapy for Cancer: Propolis and its Constituents. *J. Diet. Suppl.* **2016**, *13*, 245–268. [CrossRef]
81. Ali, A.; Ambreen, S.; Maqbool, Q.; Naz, S.; Shams, M.F.; Ahmad, M.; Phull, A.R.; Zia, M. Zinc impregnated cellulose nanocomposites: Synthesis, characterization and applications. *J. Phys. Chem. Solids* **2016**, *98*, 174–182. [CrossRef]
82. Prakash, O.; Belal, B.; Dhanik, J.; Verma, A.; Joshi, H.C.; Vivekanand, V. Biological Activities of Metal Complexes with Rutin and Bio-Conjugate of Citrus Extract. *Univers. J. Chem.* **2020**, *7*, 1–24. [CrossRef]
83. Ali, S.; Sudha, K.G.; Thirumalaivasan, N.; Ahamed, M.; Pandiaraj, S.; Rajeswari, V.D.; Vinayagam, Y.; Thiruvengadam, M.; Govindasamy, R. Green Synthesis of Magnesium Oxide Nanoparticles by Using Abrus precatorius Bark Extract and Their Photocatalytic, Antioxidant, Antibacterial, and Cytotoxicity Activities. *Bioengineering* **2023**, *10*, 302. [CrossRef]
84. Ramamurthy, C.H.; Padma, M.; Mariya Samadanam, I.D.; Mareeswaran, R.; Suyavaran, A.; Kumar, M.S.; Premkumar, K.; Thirunavukkarasu, C. The extra cellular synthesis of gold and silver nanoparticles and their free radical scavenging and antibacterial properties. *Colloids Surf. B Biointerfaces* **2013**, *102*, 808–815. [CrossRef]
85. Das, D.; Nath, B.C.; Phukon, P.; Dolui, S.K. Synthesis and evaluation of antioxidant and antibacterial behavior of CuO nanoparticles. *Colloids Surf. B Biointerfaces* **2013**, *101*, 430–433. [CrossRef]